# Efficiency and heat transport processes of low-temperature aquifer thermal energy storage systems
## new insights from global sensitivity analyses

Tas, Luka; Hartog, Niels; Bloemendal, Martin; Simpson, David; Robert, Tanguy; Thibaut, Robin; Zhang, Le; Hermans, Thomas

**DOI**
10.1186/s40517-024-00326-1

**Publication date**
2025

**Document Version**
Final published version

**Published in**
Geothermal Energy

**Citation (APA)**
Tas, L., Hartog, N., Bloemendal, M., Simpson, D., Robert, T., Thibaut, R., Zhang, L., & Hermans, T. (2025). Efficiency and heat transport processes of low-temperature aquifer thermal energy storage systems: new insights from global sensitivity analyses. *Geothermal Energy*, *13*(1), Article 2. https://doi.org/10.1186/s40517-024-00326-1

https://doi.org/10.1186/s40517-024-00326-1



RESEARCH

Open Access

# Efficiency and heat transport processes of low-temperature aquifer thermal energy storage systems: new insights from global sensitivity analyses

Luka Tas[1*], Niels Hartog[2,3], Martin Bloemendal[2,4,5], David Simpson[6], Tanguy Robert[7,8], Robin Thibaut[1,9], Le Zhang[1] and Thomas Hermans[1]

*Correspondence: luka.tas@ugent.be

[1] Department of Geology, Laboratory for Applied Geology and Hydrogeology, Ghent University, Ghent, Belgium
[2] KWR, Water Research Institute, Nieuwegein, The Netherlands
[3] Faculty of Geosciences, Utrecht University, Utrecht, The Netherlands
[4] Present Address: Department of Water Management, Delft University of Technology, Delft, The Netherlands
[5] Present Address: TNO-Dutch Geological Survey, Utrecht, The Netherlands
[6] Advanced Groundwater Techniques (AGT), Kontich, Belgium
[7] Present Address: Vivaqua, Brussels, Belgium
[8] University of Liege, Urban and Environmental Engineering, Liege, Belgium
[9] Lawrence Berkeley National Laboratory, EESA, Berkeley, CA, USA

## Abstract

Aquifer thermal energy storage (ATES) has great potential to mitigate $CO_2$ emissions associated with the heating and cooling of buildings and offers wide applicability. Thick productive aquifer layers have been targeted first, as these are the most promising hydrogeological context for ATES. Regardless, there is currently an increasing trend to target more complex aquifers such as low-transmissivity and alluvial aquifers or fractured rock formations. There, the uncertainty of subsurface characteristics and, with that, the risk of poorly performing systems is considerably higher. Commonly applied strategies to decide upon the ATES feasibility and well design standards for optimization need to be adapted. To further promote the use of ATES in such less favorable aquifers an efficient and systematic methodology evaluating the optimal conditions, while not neglecting uncertainty, is crucial. In this context, the distance-based global sensitivity analysis (DGSA) method is proposed. The analysis focuses on one promising thick productive aquifer, first used to validate the methodology, as well as a complex shallow alluvial aquifer. Through this method, multiple random model realizations are generated by sampling each parameter from a predetermined range of uncertainty. The DGSA methodology validates that the hydraulic conductivity, the natural hydraulic gradient and the annual storage volume dominate the functioning of an ATES system in both hydrogeological settings. The method also advances the state of the art in both settings. It efficiently identifies most informative field data ahead of carrying out the field work itself. In the studied settings, Darcy flux measurements can provide a first estimate of the relative ATES efficiency. It further offers a substantiated basis to streamline models in the future. Insensitive parameters can be fixed to average values without compromising on prediction accuracy. It also demonstrates the insignificance of seasonal soil temperature fluctuations on storage in unconfined shallow aquifers and it clarifies the thermal energy exchange dynamics directly above the storage volume. Finally, it creates the opportunity to explore different storage conditions in a particular setting, allowing to propose cutoff criteria for the investment in ATES. The nuanced understanding gained with this study offers practical guidance for enhanced efficiency of feasibility studies. It proves that the DGSA methodology can significantly speed up the development of ATES in more complex hydrogeological settings.

**Keywords:** Aquifer thermal energy storage (ATES), Sensitivity analysis, Uncertainty, Shallow aquifers, Optimization, Stochastic method

## Introduction

Low-temperature aquifer thermal energy storage (ATES) systems can provide heating and cooling to large buildings in a green and sustainable way saving on average 0.5 kg of $CO_2$ for every cubic meter of water extracted (Fleuchaus et al. 2018; Ramos-Escudero et al. 2021; Jackson et al. 2024). In essence, during summer, excess heat from buildings is stored in the subsurface, ready to be used for heating in winter. Conversely, cold is stored during winter to provide cooling in warmer months.

Due to its sustainable nature and wide applicability, the interest in investing in ATES is experiencing significant growth. For example, in Flanders (northern Belgium), the number of operational systems has steadily increased from 30 to 368 over the past 5 years (Databank Ondergrond Vlaanderen, n.d.). In Wallonia (southern Belgium) and Brussels (central Belgium) this growth manifests differently. There, more complex aquifers, respectively a shallow alluvial (De Schepper et al. 2020) and a fractured aquifer (De Paoli et al. 2023), were targeted for ATES despite the high uncertainty. Meanwhile, the Netherlands continue to take the lead with thousands of operational systems (Jackson et al. 2024). The growing interest has stimulated research in this field to improve understanding of the groundwater and heat transport processes occurring in the aquifer. Studies demonstrated that the thermal recovery efficiency of ATES systems depends on thermal conduction and dispersion, regional groundwater flow, and density-dependent flow (only significant at higher temperatures) (Doughty et al. 1982; Gao et al. 2017; Bloemendal and Olsthoorn 2018; Bloemendal and Hartog 2018). Consequently, the porous media heterogeneity, for instance in terms of hydraulic conductivity, can significantly impact thermal energy storage (Ferguson 2007; Bridger and Allen 2010).

Even though ATES already has a widespread implementation, uncertainties in thermal and hydraulic properties persist when aiming to make robust predictions on thermal energy storage and recovery efficiency (Hermans et al. 2019; Heldt et al. 2024; Jackson et al. 2024). This particularly presents challenges when targeting more complex, less known (deeper) aquifers where it is insufficient to rely on design standards and experience for decision-making (Winter 2004; Renard 2007; Tas et al. 2023). Currently, during the preliminary stage of ATES feasibility studies, a desktop study is carried out and in many cases it becomes apparent that wide ranges of variation are reported for several hydraulic and thermal parameters in databases and literature. To be able to efficiently design an ATES system it is crucial to have a thorough and systematic method to determine which uncertain parameters influence the recovery of the thermal energy the most. Similarly, when targeting complex settings with more uncertain parameters the potential shift of sensitive parameters needs to be understood. In this way, a field campaign can be designed that targets the sensitive parameters and thus substantially reduces the uncertainty.

Besides this, in traditional modelling the values of the uncertain parameters are often chosen based on deterministic calibration or they are set based on experience/expert judgement. This approach overlooks the fact that a calibrated model is non-unique and it fails to acknowledge that substantiated research should precede making model simplifications such as fixing model parameters to average values (Sommer et al. 2013; Farmer and Vogel 2016; Hoffmann et al. 2019; Hermans et al. 2023). To gain insights into the recoverability of stored thermal energy in a certain geological setting, this prior uncertainty should initially be considered for each parameter. This also creates the opportunity to analyze parameter distributions, potentially identifying favorable conditions for ATES and vice versa conditions that should be avoided (Renard 2007; Ferré 2017).

The stochastic approach of a distance-based global sensitivity analysis (DGSA) can tackle these issues (Farmer and Vogel 2016). It has been proven efficient in determining the model variables having the largest influence on the data and the prediction for hydrogeological applications (Scheidt et al. 2018; Hermans et al. 2019; Hoffmann et al. 2019). The DGSA methodology distinguishes itself because it allows for the models to be sufficiently general in terms of prior uncertainty so that the early conclusions can be generalized and findings widely applied (Farmer and Vogel 2016). Compared to the Morris method for sensitivity analysis, DGSA is far more flexible in terms of input and more statistically accurate in terms of output. DGSA also stands out for its computational efficiency compared to the Sobol method, a variance based way to compute sensitivity (Scheidt et al. 2018).

This paper aims to provide an original validation of the versatility and efficiency of the DGSA methodology by applying it to realistic long-term models of ATES systems in two distinct hydrogeological settings. We will simultaneously include uncertainty on the model parameters, boundary conditions and operational parameters. The first study case focuses on the traditional ATES target of a thick productive aquifer. Beyond serving to validate the methodology, it will advance the state of the art in the prediction approach of the ATES efficiency. Specifically, this study will offer a fresh perspective on how the efficiency and prediction accuracy of ATES systems relate to the choice of the uncertain variables and to the heat transport processes. The second case shifts the focus to a more complex and uncertain ATES target: a shallow alluvial aquifer characterized by a high natural hydraulic gradient. The results will offer novel insights into the influence of diverse heat transport processes on the efficiency of thermal storage in very shallow aquifers. In particular, this framework will be applied to research the influence of seasonal soil temperature fluctuations. This has so far been overlooked, disregarding a potentially significant impact. Overall, the results of the sensitivity analyses will provide a substantiated basis to streamline models in the future. By directly linking the thermal recovery efficiency to the most influential parameters, we aim to identify relations that are key to optimizing feasibility studies and decision-making processes. The broad prior uncertainty strategy, characteristic of the DGSA method and neglected in previous ATES studies, will promote the wide applicability of the findings.

## Study cases

### Case 1: thick productive aquifer

As a first case a thick sandy aquifer, capable of sustaining high flow rates, is selected. Due to its suitability, many operational ATES systems have been installed in this kind of aquifer. Therefore, from experience and literature, there is a thorough understanding of

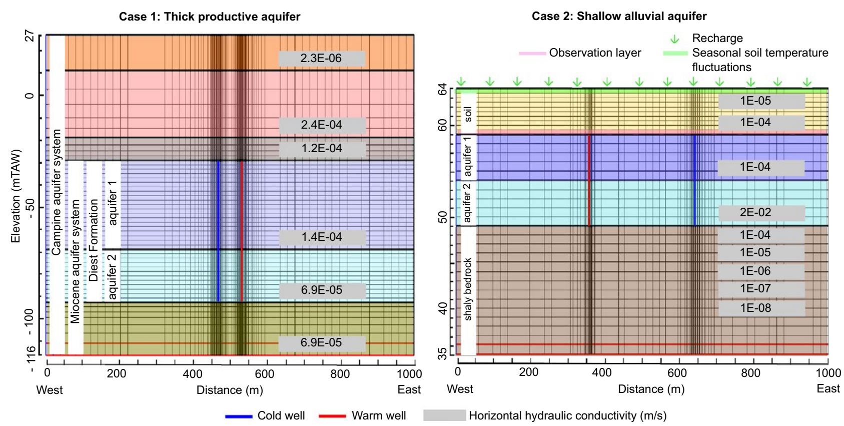


**Fig. 1** Hydrogeological representation of the two studied cases with an indication of the calibrated horizontal hydraulic conductivity values (in m/s)

the groundwater flow and heat transport processes in these prevalent settings. This prior knowledge allows us to test the methodology of DGSA for ATES and to evaluate the output with discernment.

The studied case represents an operational ATES system in Rijkevorsel, Belgium. The wells are screened in the sandy Diest Formation which extends from − 29 mTAW (meters above average sea level at low tide) to − 93 mTAW and is part of the Miocene aquifer system (Fig. 1). The upper part of this formation has a thickness of 40 m and typically has a higher hydraulic conductivity than the lower part. Above the screened interval, sandy to clayey–sandy formations are present. Below the screened interval the sandy Berchem and/or Voort Formation is present up to − 116.5 mTAW, bounded below by the Boom aquitard. Even though the case is based on a specific location, the findings of the study have broad applicability across various areas because of varying model parameters and boundary conditions in the analysis (see Sect. "The prior distribution of the cases").

### Case 2: shallow alluvial aquifer

Second, an alluvial aquifer was chosen. It is typically characterized by a high hydraulic conductivity and thus also constitutes a good target for ATES when the ambient groundwater flow is slow, as shown by De Schepper et al. (2019) and Fossoul et al. (2011). Though, the occurrence of clay lenses can locally cause lower productivity (Fossoul et al. 2011; Robert et al. 2018). A main concern, however, is a potential loss of stored thermal energy towards the atmosphere because of the shallow nature of the aquifer. This case aims to provide an improved understanding of the heat transport processes between the ground surface, which is subject to seasonal soil temperature fluctuations, and the shallow aquifer used for storage. It will also provide new insights into the suitability of shallow alluvial aquifers for ATES by relating the efficiency to design parameters, boundary conditions and model parameters.

The studied case is representative of the alluvial aquifer of the Meuse River in the region of Liege (Wallonia, Belgium) but can represent various shallow alluvial aquifer scenarios (see Sect. "The prior distribution of the cases"). There is currently one operating ATES system in this aquifer (De Schepper et al. 2020) and the area is highly investigated with field tests (Fossoul et al. 2011; Batlle-Aguilar et al. 2009; Wildemeersch et al. 2014; Klepikova et al. 2016; Hermans et al. 2019). Therefore, there is a good estimation of the (heat) transport parameters and the hydrogeology. Below the ground surface, heterogeneous soil sediments and backfill are present. The aquifer in which the wells are screened is located from + 59 mTAW to + 49 mTAW and can be divided into two layers of equal thickness (Fig. 1). The upper aquifer layer is composed of sandy gravels and the lower aquifer layer is composed of coarse clean gravels. The aquifer is bounded below by shaly bedrock with a decreasing degree of weathering downwards. Important to note is that lateral heterogeneity plays an important role in alluvial aquifers (Klepikova et al. 2016); however, the influence of this has already been thoroughly analyzed with a sensitivity analysis by Hermans et al. (2019) and is for simplicity omitted for this study.

## Methods

### Heat transport processes in the shallow subsurface

In the alluvial aquifer, thermal energy storage happens very shallow and the influence of the air temperature cannot be excluded. During winter, the warm storage area typically has a higher temperature than the air, leading to a potential energy loss towards the surface. Similarly, the cold storage area may experience energy gain. During summer this effect is reversed. Even though this phenomenon is of significant interest for understanding the thermal recovery efficiency of ATES systems in shallow aquifers, it has not yet been investigated. Nonetheless, heat losses in ATES systems have been thoroughly investigated. The main drivers in low-temperature ATES are conduction and dispersion occurring at the surface area ($A$) between the volume of stored heated groundwater and the ambient groundwater (Doughty et al. 1982; Bloemendal and Hartog 2018; Beernink et al. 2024). When the natural groundwater flow is significant, losses by displacement of the stored volume can be dominant. Generally, for the traditional range of storage conditions of ATES systems in the Netherlands, losses by conduction dominate over those by dispersion. Therefore, a fundamental parameter in analyzing these losses is the storage volume ($V$), which is the amount of water that is seasonally stored/injected with a temperature difference compared to the natural groundwater. Its shape must be as compact as possible (i.e. minimize $A/V$) to minimize heat losses. Next, it has also been demonstrated that dispersion losses are negligible through the upper and lower surfaces of confined aquifers (Beernink et al. 2024). However, case 2 does not represent a fully confined aquifer and a vertical flux through the soil layers above the aquifer must be considered. This flux can result from the ATES well operations and from the recharge that is applied on the top of the aquifer (Fig. 1).

We strived to represent the thermal energy exchange between the storage aquifer and the atmosphere by imposing a sine-shaped soil temperature profile with a monthly time discretization on top of the model (Fig. 1). Soil temperature rather than air temperature was selected as it is the surface temperature that drives the shallow subsurface thermal regime (Kurylyk et al. 2015). The variations in soil temperature will be strongly attenuated downwards in the ground because of the high heat capacity of water and the lag of the surface temperature effect also increases downward. Already at depths of more than a few meters, the variations in the top soil are negligible, which justifies why this temperature variation is typically neglected when deeper geothermal systems are modelled (Claesson and Eskilson 1988; Preene and Powrie 2009; Kurylyk et al. 2015).

Note that even though the alluvial aquifer is not fully confined, it was modelled as a confined aquifer to allow setting a fine vertical grid discretization accurately modelling the heat transport processes. As a result, the aquifer was modelled as fully saturated when in reality the groundwater table is found 3 m below the surface. This choice remains valid for the purpose of the study considering the prior uncertainty range of the top temperature and it can serve as a worst-case scenario as the unsaturated layer would act as an insulator.

## Modelling approach

### *Software*

For this project, the freely available USGS MODFLOW 2005 software (v1.12.00) was used to simulate groundwater flow (Harbaugh et al. 2017). To model the (heat) transport processes, MT3D-USGS was used (Bedekar et al. 2016), taking advantage of the analogy between the heat transport and solute transport equations as previously shown and validated (Hecht-Méndez et al. 2010; Ma and Zheng 2010; Fossoul et al. 2011; Sommer et al. 2013; Tas et al. 2023). Water density was considered constant which is a fair assumption when the temperature changes remain limited ($\Delta T < 15$ °C) (Zuurbier et al. 2013; Zeghici et al. 2015). To set up the model, ModelMuse version 5.1.1 was used as a graphical user interface (Winston 2022). To be able to run many MODFLOW-based models with different parameters efficiently for the sensitivity analysis, the Python package FloPy was used (Bakker et al. 2016; Hughes et al. 2024). Details on the influence of grid discretization and boundary conditions on the prediction as well as details on the influence of the solver settings on numerical dispersion can be consulted in the supplementary material (S1, S2).

### *Computational demand*

To overcome the substantial computational demand of running multiple simulations (see Sect. "Distance-based global sensitivity analysis"), the supercomputing facilities of Ghent University were used. The workload could be viewed as embarrassingly parallel assigning each simulation to a single CPU. Performing the tasks in this way resulted in a maximum computational requirement of ~ 72 h and ~ 8 TiB of short-term storage per case.

## Distance-based global sensitivity analysis

A sensitivity analysis provides information on the leverage of each input variable to the output and can, therefore, be of great interest during feasibility studies and decision-making processes. The knowledge of high-influential parameters can be used to determine which field data needs to be acquired to reduce the uncertainty. Furthermore, SA can reduce model complexity by fixing low-influential parameters and it can advance our understanding of the modeled system by analyzing the model response to parameter variation (Lu and Ricciuto 2020).

In previous sensitivity studies of ATES systems, only tens of distinct model realizations were chosen to draw conclusions with a structured SA (Schout et al. 2014; Poulsen et al. 2015; Bloemendal and Hartog 2018; Beernink et al. 2024; Heldt et al. 2024) or a methodology was used that requires a computationally impractical amount of runs to be accurate. For instance, Sobol's method, which is a form of GSA based on variation decomposition, is frequently employed (Jeon et al. 2015; Lu and Ricciuto 2020; Stemmle et al. 2021) but it may mis-predict the sensitivity value due to complex dependence among variables (Hoteit et al. 2023).

The distance-based global sensitivity analysis (DGSA) has been proven a computationally efficient and statistically significant method by relying on a clustering of the model response (Scheidt et al. 2018; Hermans et al. 2019; Lu and Ricciuto 2020) and its applicability for ATES systems will be validated in this paper. Essentially, the DGSA consists of first sampling model realizations from the predefined ranges of uncertainty for each parameter (i.e., the prior distribution) and generating the model output. For cases 1 and 2, 250 and 500 model realizations were sampled respectively (the number of realizations was obtained by trial and error) (Zhang et al. 2025). In this study, the output is the temperature evolution at the warm and cold ATES wells over time, recorded every 0.5 days and, in the case of the alluvial aquifer, also the energy exchange with the atmosphere. Next, the model output is classified (k-medoids/k-means) into an appropriate number of clusters, which can be verified by the Davies–Bouldin index and the mean silhouette index (Davies and Bouldin 1979; Kaufman and Rousseuw 1990; Scheidt et al. 2018). When the cluster cumulative distribution functions (cdf) of a certain parameter significantly differ, the parameter is deemed sensitive (Fenwick et al. 2014; Scheidt et al. 2018; Lu and Ricciuto 2020).

With this method, the standardized class-conditional sensitivity for each parameter but also the mean sensitivity averaged over all classes, can be determined. Similarly, the sensitivity of parameter interactions can be determined based on their conditional distributions. The application of the DGSA method was facilitated by the user-friendly pyDGSA Python package (Fenwick et al. 2014; Park et al. 2016; Perzan 2020).

#### The prior distribution of the cases

For this study, the model realizations are sampled randomly from a uniform distribution with the Latin hypercube sampling method to ensure a well-distributed coverage across the sample space (Heldt et al. 2024). The ensemble of all possible model realizations is called the prior distribution.

For case 1, the horizontal and vertical hydraulic conductivity, the total and effective porosity, the ambient groundwater flow (prescribed hydraulic gradient) and the longitudinal dispersion were varied. In case 2, the temperature of the soil (top boundary condition), the recharge and the annual storage volume were additionally varied. Only for the hydraulic conductivity a distinction was made between the upper and lower parts of the aquifers. As the natural variability in thermal properties is orders of magnitude less than the natural variability in hydraulic properties more homogeneous assumptions for heat transport are justified (Kurylyk et al. 2015). The detailed ranges of variation for both

**Table 1** Parameter values and prior definition of the thick productive aquifer

| Parameter | Unit | Initial value | | Range of variation | Package |
|---|---|---|---|---|---|
| *Hydrogeological parameters* | | | | | |
| **Horizontal hydraulic conductivity ($K_h$)** | m/s | *Aqf 1* | 1.39E−04 | U[1.00E−04 to 6.00E−04] | LPF |
| | | *Aqf 2* | 6.954E−05 | U[5.00E−05 to 2.00E−04] | |
| **Vertical hydraulic conductivity ($K_v$)** | m/s | *Aqf 1* | 4.63E−05 | U[1.00E−05 to 3.00E−04] | LPF |
| | | *Aqf 2* | 2.31E−05 | U[5.00E−06 to 1.00E−04] | |
| **Total porosity ($n_t$/*Tot. por.*)** | – | 0.35 | | U[0.25 to 0.5] | RCT, DSP |
| **Effective porosity ($n_e$/ *Eff. Por.*) ~ specific yield ($S_y$)** | – | 0.3 | | U[0.125 to 0.4] | BTN, LPF |
| Specific storage | $m^{-1}$ | 0.0001 | | – | LPF |
| **Longitudinal dispersivity ($\alpha_l$/*Long. disp*)** | m | 1 | | U[0.5 to 5] | DSP |
| Initial temperature ($T_0$) | °C | 12 | | – | SSM, BTN |
| Density water ($\rho_w$) | kg/m$^3$ | 1000 | | – | – |
| Density solid ($\rho_s$) | kg/m$^3$ | 2650 | | – | – |
| Bulk density ($\rho_b$) | kg/m$^3$ | $\rho_s \times (1 - n_t)$ | | U[1325 to 1988] | RCT |
| Thermal conductivity water ($k_w$) | W/(m°C) | 0.58 | | – | – |
| Thermal conductivity solid ($k_s$) | W/(m°C) | 2.4 | | – | – |
| Bulk thermal conductivity ($k_b$) | W/(m°C) | $k_w \times n_t + k_s \times (1 - n_t)$ | | [1.49 to 1.945] | – |
| Specific heat capacity solid ($c_s$) | J/(kg°C) | 730 | | – | – |
| Specific heat capacity water ($c_w$) | J/(kg°C) | 4183 | | – | – |
| Thermal distribution coefficient ($K_d$) | m$^3$/kg | $c_s/(c_w \times \rho_w)$ | | – | RCT |
| Effective molecular diffusion coefficient ($D_m$) | m$^2$/s | $k_b \div (n_t \times \rho_w \times c_w)$ | | U[7.12E−07 to 1.86E−06] | DSP |
| *Boundary conditions* | | | | | |
| **Prescribed hydraulic gradient (*Grad.*)** | % | 0.1 | | U[0 to 0.3] | CHD |
| *Design parameters* | | | | | |
| Injection and extraction rate ($Q$) | m$^3$/s | 2E−3 to 1E−4 (see scenario Table 3) | | – | WEL |
| Injection temperature, relative to $T_0$ ($\Delta T_{inj}$) | °C | ± 5 (see scenario Table 3) | | – | SSM |

For the parameters in bold, a random value within the range of variation was selected for the model realizations of the DGSA

**Table 2** Parameter values and prior definition of the shallow alluvial aquifer

| Parameter | Unit | Initial value | | Range of variation | Package |
|---|---|---|---|---|---|
| *Hydrogeological parameters* | | | | | |
| **Horizontal hydraulic conductivity ($K_h$)** | m/s | *Aqf 1* | 1.00E−04 | U[1.00E−05 to 1.00E−03] | LPF |
| | | *Aqf 2* | 2.00E−02 | U[1.00E−03 to 1.00E−01] | |
| **Vertical hydraulic conductivity ($K_v$)** | m/s | *Aqf 1* | 1.00E−05 | U[1.00E−06 to 5.00E−04] | LPF |
| | | *Aqf 2* | 2.00E−03 | U[1.00E−04 to 5.00E−02] | |
| **Total porosity ($n_t$ /*Tot. por.*)** | – | | | U[0.25 to 0.5] | RCT, DSP |
| **Effective porosity ($n_e$/ *Eff. por.*) ~ specific yield ($S_y$)** | – | 0.3 | | U[0.125 to 0.4] | BTN, LPF |
| Specific storage | $m^{-1}$ | 5.00E-02 | | – | LPF |
| **Longitudinal dispersivity ($\alpha_l$/*Long. disp.*)** | m | 5 | | U[0.5 to 5] | DSP |
| Initial temperature ($T_0$) | °C | Average of $T_s$ | | – | SSM, BTN |
| Density water ($\rho_w$) | kg/m$^3$ | 1000 | | – | – |
| Density solid ($\rho_s$) | kg/m$^3$ | 2650 | | – | – |
| Bulk density ($\rho_b$) | kg/m$^3$ | $\rho_s \times (1 - n_t)$ | | U[1325 to 1988] | RCT |
| Thermal conductivity water ($k_w$) | W/(m°C) | 0.58 | | – | – |
| Thermal conductivity solid ($k_s$) | W/(m°C) | 3 | | – | – |
| Bulk thermal conductivity ($k_b$) | W/(m°C) | $k_w \times n_t + k_s \times (1 - n_t)$ | | [1.79 to 2.395] | – |
| Specific heat capacity solid ($c_s$) | J/(kg°C) | 878 | | – | – |
| Specific heat capacity water ($c_w$) | J/(kg°C) | 4183 | | – | – |
| Thermal distribution coefficient ($K_d$) | m$^3$/kg | $c_s/(c_w \times \rho_w)$ | | – | RCT |
| Effective molecular diffusion coefficient ($D_m$) | m$^2$/s | $k_b \div (n_t \times \rho_w \times c_w)$ | | U[8.56E−07 to 2.29E−06] | DSP |
| *Boundary conditions* | | | | | |
| **Prescribed hydraulic gradient (*Grad.*)** | % | 0.1 | | U[0 to 0.2] | CHD |
| **Recharge** | m/s | 2.00E-09 | | U[5.29E−09 to 8.46E−09] | RCH |
| **Soil temperature ($T_s$)** | °C | Winter (*T winter*) | 4 | U[2.5 to 8] | SSM |
| | | Summer (*T zomer*) (May–October) | 16 | U[15 to 20.5] | |
| *Design parameters* | | | | | |
| **Annual storage volume (*V*)** | m$^3$ | 200,000 | | U[12,500 to 200,000] | WEL |
| Injection temperature, relative to $T_0$ ($\Delta T_{inj}$) | °C | 5 | | – | SSM |

For the parameters in bold, a random value within the range of variation was selected for the model realizations of the DGSA

cases can be consulted in Tables 1 and 2 and a clarification on the choice of the lower and upper limits is provided in the supplementary materials (S3).

The vertical hydraulic conductivity was determined as a ratio from the horizontal hydraulic conductivity with *Kh/Kv* ratios varying from 2 to 10. Similarly, the effective porosity was calculated as a percentage of the total porosity, ranging from 50 to 80%.

The horizontal and vertical transversal dispersion were set at 1/10 and 1/100 of the longitudinal dispersion, respectively.

## Assessment framework

### *Modelling scenarios*

The model of case 1 mimics, in terms of flow rate and injection temperature, the functioning of the operational ATES system. The choice was made to use the first 7 months of monitoring data, repeated 3 times, for the DGSA. The monitoring data was considered with a monthly time discretization (half-monthly for October) and simplifications were made because, in reality, the ATES system could quickly switch between heating and cooling modes when it was required. Mimicking the operational system means that the storage volume in cooling mode did not equal the storage volume in heating mode (Table 3).

For case 2, a 2-year simulation was used starting with the cooling season (typically the first of May). The annual storage volume in Table 2 corresponds to the total amount of water that is stored in both the warm and cold storage area each year. Heat was stored during the initial 180 days of each year and cold was stored during the subsequent 180 days, employing a synthetic sine-shape profile with a monthly time discretization for the flow rate of the system. This means that the system is balanced. The injected volume equals the extracted volume during the subsequent season.

### *Thermal recovery efficiency*

Once the sensitive parameters were determined, their values were associated with the thermal recovery efficiency of the ATES system. This is often used as the main indicator of the overall energy savings of ATES systems and it is both affected by storage specifics and site-specific hydrogeological conditions (Bloemendal and Hartog 2018). The thermal recovery efficiency can be calculated for each season as the percentage of thermal energy that can be extracted from the energy that was stored in the previous cycle (Duijff et al. 2021; Tas et al. 2023; Beernink et al. 2024):

**Table 3** Scenario for the DGSA of the ATES system in the thick productive aquifer based on monitoring data available from the operational system in Rijkevorsel

| Stress period (–)—duration (days) | Flowrate cold well ($m^3/s$) | Flowrate warm well ($m^3/s$) | Injection temperature warm well (°C) | Injection temperature cold well (°C) |
|---|---|---|---|---|
| 1–31 | − 0.002329 | 0.002329 | 14.34 | – |
| 2–31 | − 0.001254 | 0.001254 | 14.61 | – |
| 3–30 | − 0.000136 | 0.000136 | 16.92 | – |
| 4–11 | − 0.000200 | 0.000200 | 14.33 | – |
| 5–20 | 0.000323 | − 0.000323 | – | 9.01 |
| 6–30 | 0.000451 | − 0.000451 | – | 8.49 |
| 7–31 | 0.000552 | − 0.000552 | – | 7.76 |
| 8–31 | 0.000948 | − 0.000948 | – | 7.20 |

This scenario is repeated 3 times to represent 3 full operational cycles

$$\eta\text{th} = \frac{E_{\text{ex}}}{E_{\text{in}}} = \frac{\int_0^t Q_{\text{ex}} c_{\text{w}} \Delta T \, dt}{\int_0^t Q_{\text{in}} c_{\text{w}} \Delta T \, dt},$$

where $E_{ex}$ and $E_{in}$ (kWh) are the extracted and injected energy, $Q_{ex}$ and $Q_{in}$ ($m^3/h$) the total extraction and injection flow rate of the system, $c_w$ the specific heat capacity of water (1.16 kWh/$m^3$K), $\Delta T$ (°C) is the absolute temperature difference between the injected/extracted water and the ambient groundwater temperature of the aquifer, and $t$ (h) is time.

#### *Vertical thermal energy exchange*

To explore the influence of seasonal soil temperature fluctuations on the efficiency of shallow ATES systems, the vertical thermal energy exchange between the storage aquifer and the soil was determined. As such, our aim is to quantify the vertical thermal losses/gains. Conceptually, the soil layer of 0.5 m thickness, right above the aquifer, was used as an observation layer (Fig. 1). In every cell of this layer, the vertical mass flux $Q_v$ ($m^3/h$) and the absolute temperature difference between with the natural groundwater temperature $\Delta T_{abs}$ (°C) were analyzed to derive the vertical energy exchange (Exchange, kWh) per season:

$$E_{\text{exchange}} = \int_0^t Q_{\text{v}} c_{\text{w}} \Delta T_{\text{abs}} dt.$$

When the energy exchange is calculated for each cell, the total energy exchange through the entire layer or through the areas right above the cold and warm storage can be determined. Subsequently, a DGSA was done based on the calculated vertical energy exchange per season. Based on these results, the influential parameters can be associated with the thermal energy exchange or the thermal recovery efficiency. Furthermore, the necessity was assessed of accurately reflecting shallow soil temperature variations in alluvial aquifers with sine-shaped temperature profiles in ATES models. This was accomplished by comparing the vertical energy exchange results to the output of models where the top boundary condition had a constant temperature, equal to the natural average groundwater temperature.

## Results

### Case 1: thick productive aquifer

#### *Parameters sensitive to the temperature evolution over time*

The temperature difference between both wells is used for the DGSA. To determine the sensitive parameters, first, the model responses were clustered into three classes (Fig. 2A). The k-medoids clustering method was used and it was confirmed that the k-means method does not yield a different outcome. The derived classes represent model realizations exhibiting generally high/medium/low temperature differences, corresponding to field conditions which lead to the most/less/least efficient ATES systems in this type of study area.

The mean sensitivity reveals that the natural hydraulic gradient and the vertical and horizontal hydraulic conductivity of the upper aquifer layer are the sensitive parameters (Fig. 2B, C). The conductivity of the lower aquifer layer is not sensitive. This

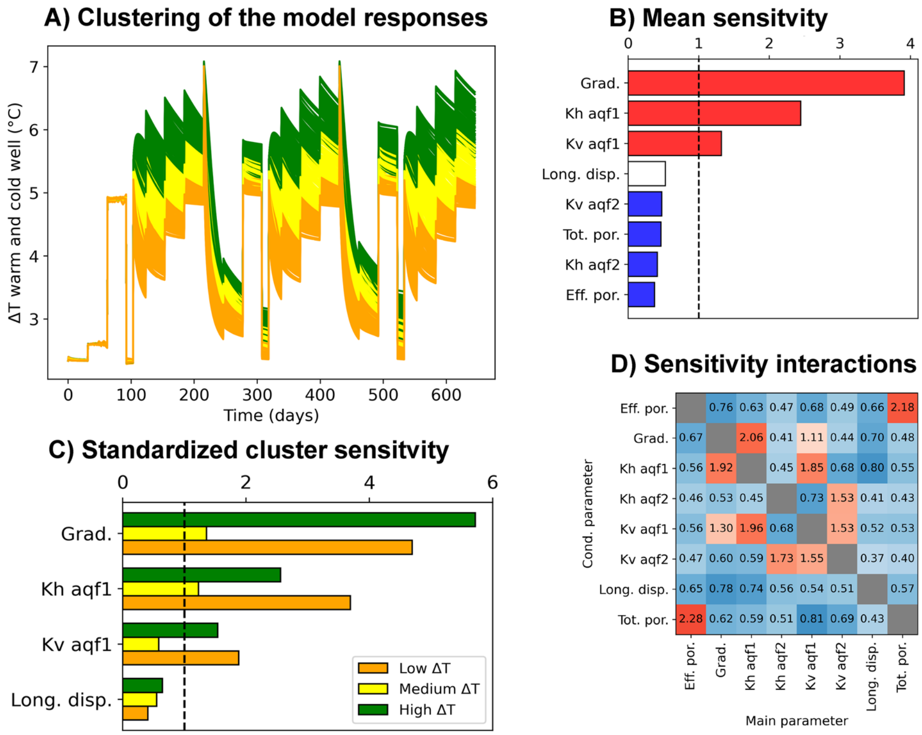


**Fig. 2** DGSA results of case 1. **A** Temperature evolution with time in the thick productive aquifer clustered into 3 classes, **B** the mean standardized sensitivity for all parameters, **C** the cluster standardized sensitivity of the top 4 influential parameters, **D** the standardized sensitivity of interactions between parameters

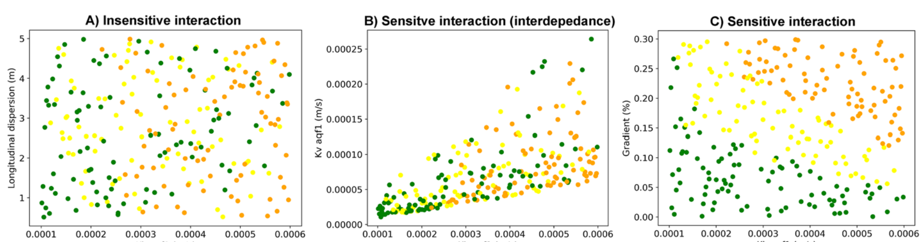


**Fig. 3** Parameter distribution clarifying the type of parameter interactions ranging from insensitive (**A**), to apparently sensitive (**B**) and truly sensitive (**C**) interactions. The model realizations are colored according to their respective cluster: green, yellow, orange for the high, medium, low efficiency clusters

aligns with our expectations because the lower aquifer contributes less to the total flow rate of the ATES system.

Nevertheless, if an insensitive parameter contributes to a sensitive interaction with another parameter, it should still be considered for further analysis. The interaction matrix in Fig. 2D highlights interactions between the total and effective porosity and between horizontal and vertical hydraulic conductivity for both aquifer layers which were not further explored as these are parameters that were linked to each other in the prior (Table 1). This is also visible in Fig. 3B as the parameter distribution does not expand across the entire 2D parameter space. Next to this, also interactions between the gradient and the hydraulic conductivity of the upper aquifer layer

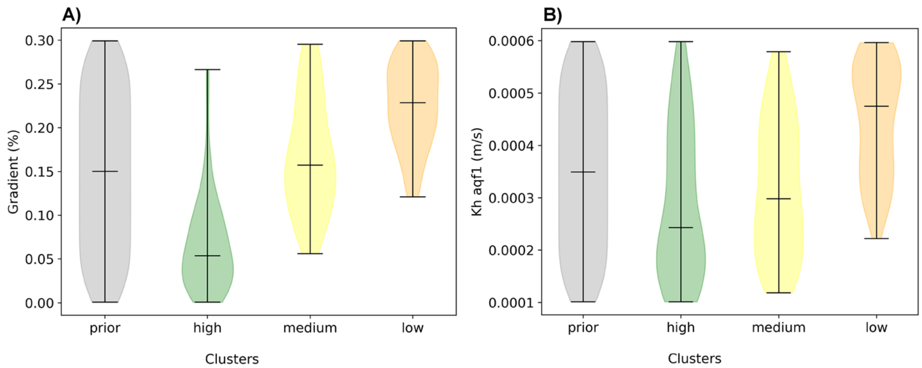


**Fig. 4** Parameter distribution of the prior and the classes of case 1 for (**A**) the natural hydraulic gradient and (**B**) the horizontal hydraulic conductivity of aquifer 1

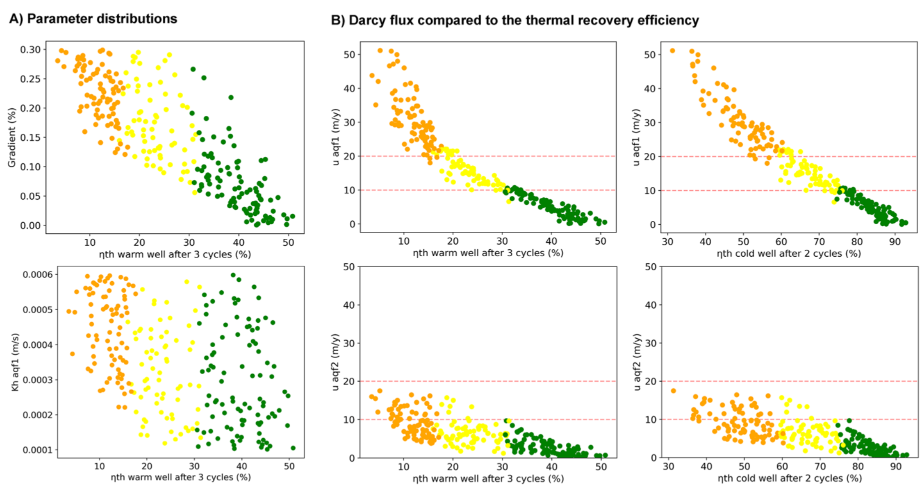


**Fig. 5** **A** Parameter distributions of the horizontal hydraulic conductivity and the natural hydraulic gradient showing a general trend but a broad uncertainty (spreading) on the thermal recovery efficiency. **B** Illustration of the link between the Darcy flux (*u*) and the thermal recovery efficiency in case 1 for both the warm and cold well in aquifer 1 and aquifer 2. Model realizations are colored according to their respective cluster

become apparent. Plotting the parameter distribution of these two variables against each other reveals a distinct boundary between the classes (Fig. 3C). If the interaction between two parameters is insensitive, clusters are mixed (Fig. 3A).

Figure 4 gives more insights into the sensitive parameter distribution within the classes. It confirms that ATES systems in study areas characterized by a high natural gradient and a high hydraulic conductivity in the main production layer are the least efficient (Fig. 4A, B). This combination facilitates the movement of stored volume away from the extraction area due to the natural groundwater flow, reducing the system's effectiveness. Nevertheless, Fig. 4 also illustrates an overlap of cluster ranges meaning that knowledge of these individual parameters is not sufficient to reduce the uncertainty on the energy efficiency of the ATES system, but that both must be considered together.

### *Thermal recovery efficiency*

To narrow down the conditions for optimal recovery, we aimed to link the thermal recovery efficiency of the ATES system to the sensitive parameters.

The thermal recovery efficiency was calculated for each season. As the efficiency of ATES systems increases with time, especially in the first seasons, the last season of extraction was selected for comparison with the natural hydraulic gradient, the horizontal hydraulic conductivity and the Darcy flux (Fig. 5). Figure 5A illustrates that when a single sensitive parameter is considered there is a broad spreading or a high uncertainty regarding the efficiency, as Fig. 4 also indicates. This is opposed to Fig. 5B where the Darcy flux, a combination of the two sensitive parameters, exhibits a distinct link with the thermal recovery efficiency. Figure 5B also shows that there is a significant difference in thermal recovery efficiency between the warm and cold wells for case 1. This owes to the total flow rate of the system which is significantly lower in winter season than in summer season. Apart from this, the results of the sensitive aquifer 1 show that the distinctions between the low and medium and medium and high classes correspond to a Darcy flux of 20.5 m/y and 9.5 m/y respectively, for both the warm and the cold well.

When the same procedure is applied to the insensitive aquifer 2, the limits do not correspond to the class boundaries anymore (Fig. 5B). This is attributed to the fact that only the sensitive parameters facilitate the clustering of the model response because only these parameters influence the model response significantly. Therefore, using the same clusters and limits to insensitive parameters may not produce meaningful results.

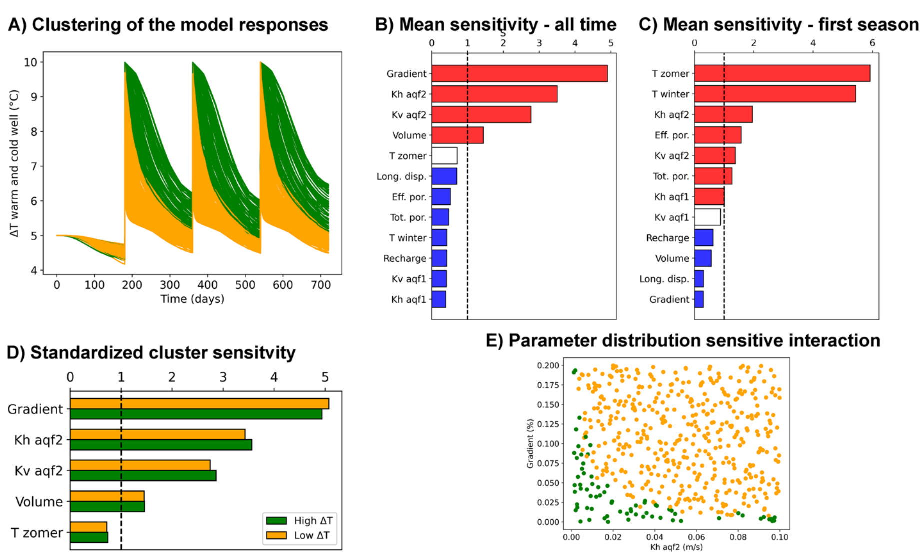


**Fig. 6** DGSA results of the temperature evolution with time of case 2. **A** Clustering of the model response into two classes, **B** mean standardized sensitivity of the full model response for all parameters, **C** mean standardized sensitivity of the first season of the model response for all parameters, **D** cluster standardized sensitivity of the top 5 influential parameters, **E** parameter distribution of the sensitive interaction between the gradient and the horizontal hydraulic conductivity of aquifer 2

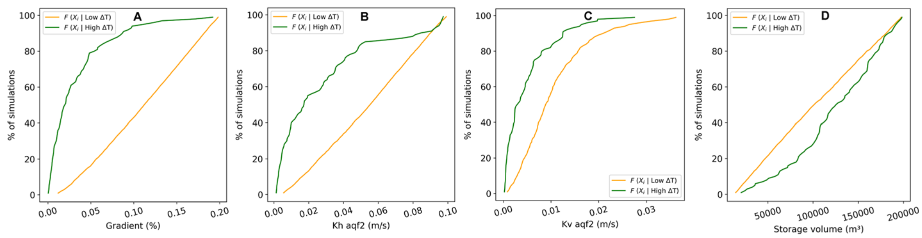


**Fig. 7** Cumulative distribution functions (cdf's) of case 2 for (**A**) the natural hydraulic gradient, the horizontal (**B**) and vertical (**C**) conductivity of aquifer 2, and (**D**) the annual storage volume. The model realizations are colored according to their respective cluster: green, and orange for the high and low efficiency clusters

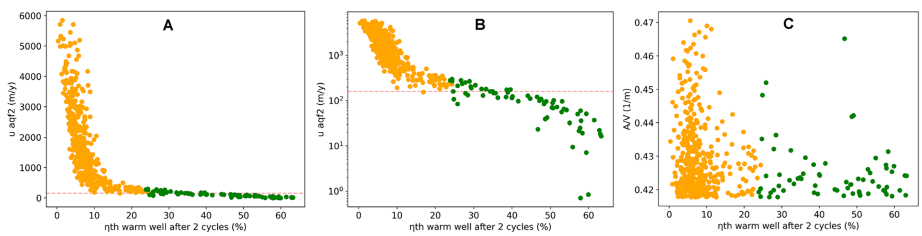


**Fig. 8** Illustration of the link between the Darcy flux and the thermal recovery efficiency in aquifer 2 of case 2 on a linear (**A**) and logarithmic scale (**B**). **C** Plot of the thermal recovery efficiency in function of the *A/V*-ratio. Model realizations are colored according to their respective cluster

## Case 2: Shallow alluvial aquifer

### *Parameters sensitive to the temperature evolution over time*

The clustering of the model responses resulted in two classes, distinguishing between a generally high and low temperature difference, which represent field and/or operational conditions leading to the most and least efficient ATES systems. They had significantly different sizes, with approximately 420 and 80 samples, necessitating the double amount of samples to obtain statistically significant results (Fig. 6A).

The gradient and the vertical and horizontal conductivity of the most transmissive aquifer layer also emerge as the most important parameters influencing the temperature evolution over time. In addition, the annual storage volume was identified as a sensitive parameter highlighting the significant role of this operational parameter in the system performance (Fig. 6B, D). Interestingly, the clustering for the three last seasons yielded desirable results while no clear distinction between classes is observed in the first season (Fig. 6A). This is because the first season only represented injection at a constant temperature and extraction of groundwater at its natural temperature, influenced by the soil temperature in summer season. The following seasons represent the actual recovery of stored thermal energy as is the case for an operating ATES system. To acknowledge this difference a separate DGSA was carried out for the first season which indeed showed that, initially, the top boundary condition has the most significant influence on the model responses (Fig. 6C). Also, the total and effective porosity and the hydraulic conductivity of aquifer 2 are sensitive parameters for the first season demonstrating their importance for heat transport in the shallow subsurface.

The interactions between the parameters remained consistent with those of case 1 (Fig. 6E) and the cdf's in Fig. 7 also confirm that generally a low natural gradient and hydraulic conductivity in the lower range lead to more efficient systems. The cdf's also reveal that model realizations with larger annual storage volumes retain higher temperature differences (Fig. 7D).

#### *Thermal recovery efficiency*

Figure 8 links the thermal recovery efficiency of the ATES system under different field and operational conditions to the Darcy flux. A Darcy flux of approximately 160 m/y is the demarcation (Fig. 8A, B) between both classes. Even though the storage volume was identified as sensitive to the temperature evolution over time in the alluvial aquifer, no useful relationship could be derived when comparing the A/V ratio to the thermal energy recovery (Fig. 8C).

#### *Parameters sensitive to the thermal energy exchange*

An additional DGSA was carried out on the total energy exchange within a small area of 20 m by 20 m above the warm and cold wells separately, offering perspectives on the dynamics directly above the storage area. Negative values denote an energy gain for the storage area, whereas positive values indicate a loss. This model response was clustered into two classes, the high class corresponding to higher energy gains/losses and the low class corresponding to lower energy gains/losses (Fig. 9A, B). The sample distribution across the two classes differs from the classification based on the temperature evolution over time (Fig. 6).

The conductivity values of the most transmissive aquifer layer are again sensitive parameters as well as the annual storage volume (Fig. 9C). In addition, there is a sensitive interaction between the horizontal hydraulic conductivity of aquifer 2 and the volume (Fig. 9D). This is reflected in the parameter distribution in Fig. 9E revealing that

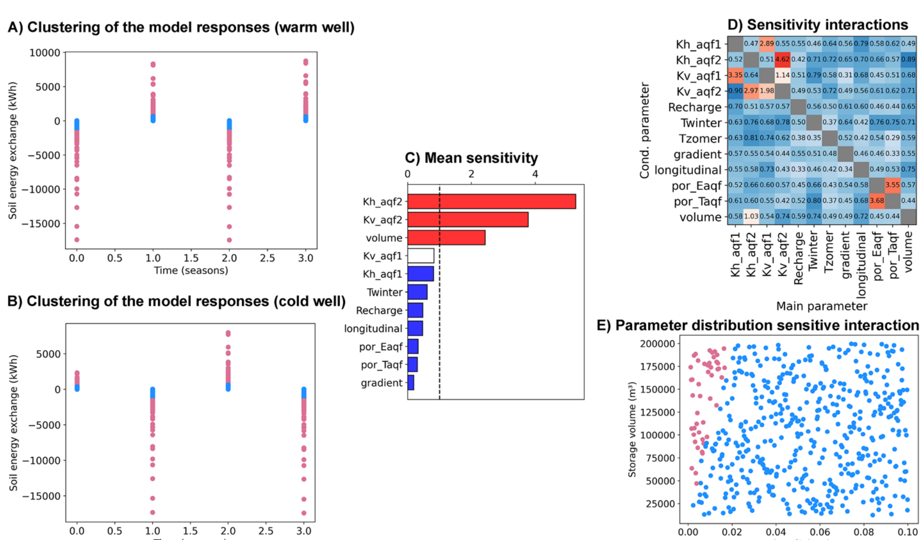


**Fig. 9** DGSA results of the thermal energy exchange (20 m by 20 m around wells) in each season of case 2. Clustering of the model response in the warm (**A**) and cold well (**B**). **C** Mean standardized sensitivity of all parameters, (**D**) sensitivity of the interactions, and (**E**) parameter distribution of the sensitive interaction between the annual storage volume and the horizontal hydraulic conductivity of aquifer 2

model realizations with a lower conductivity of aquifer 2 and a high storage volume have significantly higher losses/gains. This might be explained by an increased vertical flow in the neighborhood of the wells. The natural gradient was no longer identified as a sensitive parameter, which aligns with the expectations when analyzing a small area around the wells. The DGSA of the model realizations with a constant soil temperature equal to the initial temperature of the aquifer show the same results (S4). It confirms that the soil temperature is not a sensitive parameter for the energy exchange above the storage area of the ATES wells.

#### *Influence of seasonal soil temperature fluctuations on shallow ATES*

Figure 9A, B shows that there are not only losses of energy towards the overlying layer but also gains. It also reveals that, for shallow aquifers, this vertical energy exchange is not dependent on seasonal soil temperature fluctuations but it is dominated by the cyclic functioning of the ATES system itself (Fig. 9C). The amount of energy exchange in Fig. 9A is also negligible in comparison to the power produced by the ATES system (which is maximum 800,000 kWh for the model realizations). This insignificance is further confirmed by the fact that vertical heat losses in one season are counterbalanced by gains in the following season. This means that also for shallow alluvial aquifers, not overlain by an aquitard, the vertical heat losses are negligible compared to the lateral losses within the storage aquifer itself.

To determine whether it is worth applying a detailed sine-shape profile reflecting the monthly soil temperature instead of a constant value, the thermal recovery efficiency of both options was compared for each sample. Figure 10 shows that applying a constant temperature at the top results in a consistent underestimation of the efficiency of the ATES system. The difference in recovery efficiency is up to 10% but decreases significantly to a maximum of 6% in the second year of operation. There is no link between the predicted efficiency of the ATES system and the difference in efficiency in both scenarios.

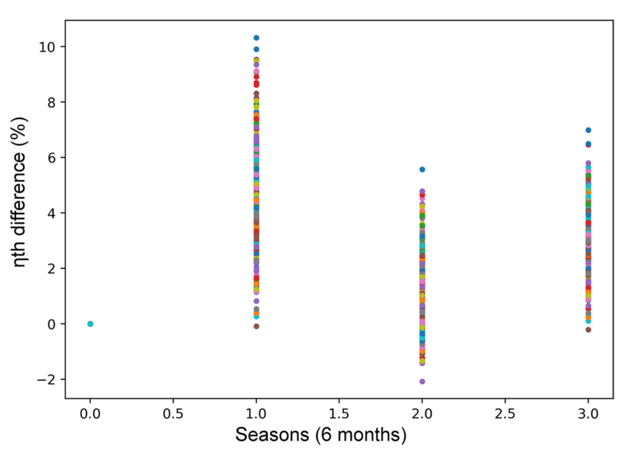


**Fig. 10** Difference in thermal recovery efficiency for each model realization when imposing seasonal soil temperature variations instead of imposing a constant top temperature equal to the initial aquifer temperature

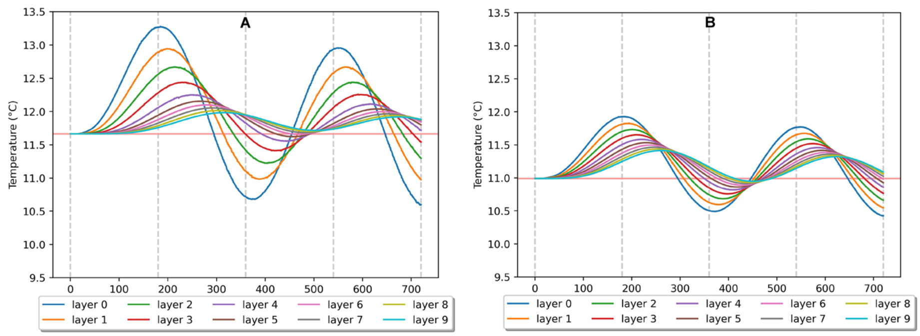


**Fig. 11** Natural temperature evolution with time and depth for one model realization of each cluster (**A**, **B**). No ATES system was implemented. A sine-shaped temperature profile was imposed reflecting the seasonal soil temperature variations

The observed difference in efficiency is attributed to the influence of the seasonal fluctuation of the soil temperature on the storage aquifer. To better understand this effect, one sample of each cluster was selected and simulated with the sine-shape top boundary condition but without the ATES system. The results clearly show that there are temperature fluctuations within the aquifer itself (Fig. 11A, B). These fluctuations have an increasing lag and are decreasing in amplitude with depth. This effect results in a slightly higher temperature during the entire year in the lower part of the alluvial aquifer. In the upper part of the alluvial aquifer, it results in a generally higher or lower temperature with the switch occurring roughly in the middle of each 6-month season.

The fact that there is a difference in recovery efficiency when applying different top boundary conditions even though the sensitivity analyses indicated no sensitivity could have been anticipated. The sensitivity analysis of the temperature evolution over time in the first season of operation already indicated this (Fig. 6C). Water was extracted from the cold well area with a different temperature from the initially imposed value which implied that the varying soil temperature influenced the natural aquifer temperature and thus also the ATES efficiency.

## Discussion

### Implications for modelling ATES systems

The outcome of the DGSA shows that several model parameters are insensitive to the long-term temperature evolution over time in the warm and cold wells. Specifically, these include the total and effective porosity, the longitudinal dispersivity, the recharge, as well as vertical and horizontal hydraulic conductivity of the least permeable aquifer layer. The total porosity impacts heat transport by conduction through the molecular diffusion coefficient. The longitudinal dispersivity, together with advective transport facilitated by the effective porosity, contributes to heat transport through dispersion processes. Literature reports wide variations in these parameters owing to the diverse nature of aquifers and the questionable accuracy of the estimation through field tests, stemming from uncertain data quality and limited data density (Winter 2004; Renard 2007; Fu and Jaime 2009; Beernink et al. 2022). In shallow aquifers, the recharge rate is also arguable and challenging to estimate due to temporal and spatial variations and dependencies of the runoff on factors such as the percentage of hardened surface, the initial soil saturation, and the rain intensity (Ajami 2021). Despite considering a broad uncertainty range in the prior, the insensitivity of these variables implies that they can be fixed to average values without significantly influencing the predicted ATES efficiency. Moreover, the consistency of insensitive variables across both cases and previous less general sensitivity studies by Fossoul et al. (2011), Hermans et al. (2018) and Schout et al. (2014) further strengthens this conclusion, affirming the feasibility of using average values to streamline modelling without significantly compromising on prediction accuracy.

In Figs. 5B and 8B, the Darcy flux (a combination of the two main sensitive parameters) was compared to the efficiency. It shows a more refined relationship than when comparing just one parameter to the efficiency (Fig. 5A). However, there is still a significant spreading around the trend. This is because the efficiency is a result of the combinations of all parameters, also less sensitive ones. Even though these parameters are insensitive, they still slightly contribute to the variability of the efficiency. In other words, the spread represents the possible error/uncertainty associated with the model simplification of fixing insensitive parameters to average values.

Furthermore, this study reveals that adopting a top boundary condition mirroring seasonal soil temperature fluctuations impacts the average ambient aquifer temperature up to a depth great enough to impact the thermal recovery efficiency of a shallow ATES system. This influence arises from imposing a consistent 5 °C temperature difference between injected water and the natural ambient aquifer temperature while this study shows that the natural aquifer temperature will actually change by the top boundary condition. The analyses with the constant top temperature boundary condition (and thus a constant natural groundwater temperature) cause the efficiency to be systematically underestimated with only a few percents. In this context, it is important to note that the models assessed worst-case scenarios and in reality, an unsaturated layer is present acting as an insulator, substantially attenuating the impact of the seasonal soil temperature variations. Hence, assuming a constant soil temperature during shallow ATES system modelling is justified. This choice might slightly underestimate the thermal recovery efficiency and is, therefore, conservative.

Nevertheless, this modelled variation in efficiency underscores the importance of accounting for and estimating the initial temperature and temperature fluctuations within the aquifer when assessing the ATES efficiency. These variations might for instance arise from imbalanced ATES systems, leading to overall heating or cooling of the aquifer. In addition, the presence of urban heat islands could exert an influence, both on shallow and deep layers (Luo and Asproudi 2015; Schweighofer et al. 2021; Hemmerle et al. 2022; Patton et al. 2024). To our knowledge, this is not yet widely taken into account during feasibility studies for ATES. By acknowledging and understanding the relevant temperature dynamics within the aquifer, ATES system predictions can be refined to better capture real-world conditions and possibly optimize efficiency.

Sensitivity results should always be interpreted considering the sampling method of the prior. For instance, the vertical hydraulic conductivity only emerges as sensitive because it is defined as a ratio from the horizontal hydraulic conductivity in the prior, which is revealed by analyzing the interactions (Fig. 3B). Furthermore, the two studied settings are based on existing cases but the broad uncertainty ranges allow for a wider applicability. The results can be safely extrapolated for other cases that have (estimated) parameter values within the ranges of Tables 1 or 2. For a different hydrogeological setting, outside the studied ranges, a separate DGSA study should be carried out. As such, the broad prior uncertainty strategy proves its value by expanding (while clearly delimiting) the applicability of the findings.

### Implications for ATES feasibility studies

This study identifies the hydraulic conductivity, natural hydraulic gradient and annual storage volume as sensitive parameters which is consistent with the expectations. Knowledge of the sensitive parameters can help optimize future feasibility studies for ATES by focusing field tests to obtain information on parameters that will reduce the uncertainty the most. Accordingly, flux measurements are likely the most efficient, cost-effective and logistically simple strategy. This was confirmed by Hermans et al. (2018) who studied heat tracer tests in the context of an ATES study and revealed that they are efficient in refining the prediction primarily only because of their sensitivity to the hydraulic conductivity and natural gradient (Darcy flux).

Novel threshold values for Darcy flux are identified which can be used to classify future potential ATES systems into more efficient, less efficient, and least efficient categories before having to carry out a more detailed case-specific feasibility study. In addition, the DGSA method with a broad prior uncertainty allows us to gain general insights into the conditions where recovery efficiency will be optimal. It is important to keep in mind that when assessing different classes of thermal recovery efficiency for ATES systems, they should be viewed as relative indicators of the efficiency rather than conclude on absolute values of the expected thermal recovery efficiency. This is because the efficiency of ATES systems typically increases over time as not all injected thermal energy is recovered during the extraction phase. It is only after a certain time of operation ($\pm 5$ years) that a dynamical equilibrium is achieved. The supplementary materials provide a validation of the results based on the considered shorter simulation time of 3 and 2 cycles for cases 1 and 2 respectively (S5). Moreover, the Darcy flux thresholds only offer a relative indication of efficiency because the calculation of the thermal recovery efficiency is dependent on the flow rate. The flow rate fluctuates based on the demand and is, therefore, not necessarily equal in the summer and winter seasons.

For case 1, the parameter distributions indicate that when the horizontal hydraulic conductivity and gradient are below 2.2E−4 m/s and 0.12%, the least efficient storage conditions (within the considered range of uncertainty) will always be avoided (Fig. 4). Still, even for a higher conductivity and/or gradient the ATES system can be highly efficient, as illustrated by the overlap of the parameter ranges of the 3 clusters. In that regard, a Darcy flux measurement is more informative compared to an estimation of the gradient/hydraulic conductivity alone. Then, it is sufficient to determine whether the estimated darcy flux is lower than 9.5 m/y, higher than 20.5 m/y or in between both thresholds to get a relative idea of the thermal recovery efficiency that can be expected. Nevertheless, even the least efficient class of ATES systems still holds the potential for significantly contributing to mitigate greenhouse gas emissions compared to conventional heating and cooling systems. They would still outperform alternatives like air source heat pumps. This suggests that the investment in ATES systems at less optimal locations can still be justified, up to a certain extent, given these advantages (Tas et al. 2023).

When examining case 2, the threshold value of the Darcy flux should rather be viewed as a decisive boundary in determining the feasibility of ATES systems. The least efficient cluster already exhibits a very low thermal recovery efficiency, and it is important to point out that this study did not include lateral heterogeneity in the models which would likely further reduce the efficiency of the system (Sommer et al. 2013; Bloemendal and Hartog 2018). Therefore, ATES systems in shallow alluvial aquifers with a natural Darcy flux exceeding 160 m/y are not advised when aiming for sustainable development of the subsurface in the long term. The results also show that there are only a few favorable combinations of natural gradient and hydraulic conductivity within the gravel layer, indicating a generally lower efficiency of ATES systems in such aquifers (Fig. 6E). To enhance the system performance in these conditions it is recommended to rather target the upper part of the alluvial aquifer with lower permeability while excluding the lower gravel part, where the natural gradient has a greater adverse impact on the efficiency. This can also be derived when comparing the results of Hermans et al. (2018, 2019) which each targeted a different layer of the alluvial aquifer. Lateral heterogeneity present in alluvial aquifers could also be of advantage by adapting the location for storage to make optimal use of clay lenses that can act as hydraulic barriers (Sommer et al. 2013; Possemiers et al. 2015). In addition, as suggested by Bloemendal and Olsthoorn (2018), aligning multiple warm and cold wells in these conditions in the direction of groundwater flow can help recover the thermal energy that would otherwise be lost due to the high natural Darcy flux. Despite the existing uncertainty, alluvial aquifers remain interesting targets for ATES due to their high productivity and low investment cost (shallow drillings) (Robert et al. 2018). Nevertheless, when designing the ATES system attention should be paid to avoid inundation because the water table is close to the ground surface.

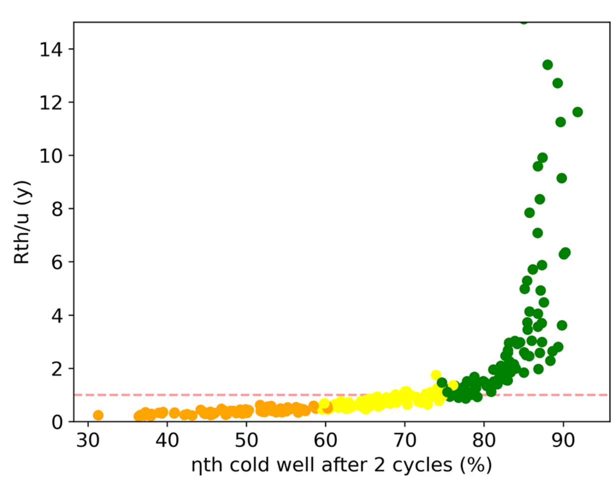


**Fig. 12** Relation between the Rth/u-ratio and the thermal recovery efficiency with indication of the 1-year line which coincides with the 80% efficiency threshold established by Bloemendal and Hartog (2018). Model realizations are colored according to their respective cluster

It must be emphasized that the derived demarcations linking the Darcy flux to the relative efficiency of ATES systems are applicable specifically for target aquifers falling within the initially defined ranges of the sensitive parameters and it should be pointed out that the thickness of the target aquifers (and for case 1 also the storage volume) remained constant throughout the analyses. While conductivity values could potentially be translated to transmissivity, altering the aquifer thickness (or the length of the filter) would inevitably impact the geometry of the storage volume. This, in turn, affects the extent of the thermal losses and consequently the thermal recovery efficiency. Even though the aquifer thickness and, for case 1, the storage volume would be influential parameters they were not included in this study for simplicity. Including these parameters will likely further confirm the outcomes of previous work by Bloemendal and Hartog (2018). As a comparison, plotting the ratio of the thermal radius of influence (*Rth*) and the Darcy flux (*u)* against the thermal recovery efficiency illustrates that the boundary between the high and medium cluster is located around 1 year (Fig. 12). This is the same as the 80% efficiency line identified by Bloemendal and Hartog (2018).

Below this threshold, small changes in the ratio cause large changes in the efficiency meaning that *Rth* has a significant impact on the order of magnitude of the thermal losses for the medium and low clusters. This implies that, for those conditions, losses due to displacement of the storage volume by the ambient groundwater flow velocity are dominant over conduction and dispersion losses. The losses can be more limited when aiming for a less elongated geometry of the storage volume. In the high cluster, dispersion and conduction losses dominate and the efficiency could be further optimized by minimizing the *A/V* ratio following the guidelines by Bloemendal and Hartog (2018). However, this study does not focus on generating guidelines to optimize ATES well design and recovery efficiency of a single ATES system. Instead, the results provide guidance for decision-making on the feasibility of ATES in the discussed hydrogeological settings, keeping in mind that the storage volume and screened length are operational parameters which could be optimized using the existing guidelines but which in practice also often rely on the available subsurface space, drilling and installation costs, and the energy demand (Bloemendal et al. 2018).

#### Future outlook on the application of DGSA and uncertainty quantification for ATES

In Flanders, the initial assessment of the potential for ATES systems is currently mapped according to the transmissivity (AGT (Advanced Groundwater Techniques), 2015). This classification prioritizes the ability to reach a high flow rate and does not indicate the expected efficiency of the ATES system. Based on the insights of this study, it could be beneficial to systematically update this suitability map with Darcy flux measurements. This could offer stakeholders a preliminary estimate of the expected recovery efficiency before committing to and investing in more detailed feasibility studies. Similarly, the existing licensing framework for ATES in Flanders lacks criteria for the minimum efficiency and energy balance that should be reached even though it is of crucial interest when aiming for an optimal distribution of subsurface activities and a sustainable use of the subsurface (Bloemendal et al. 2018; Compernolle et al. 2022). The link between the Darcy flux and the thermal recovery efficiency that was revealed with the sensitivity analysis might have a practical use in this context as well. More specifically, the Darcy flux values could provide substantiated thresholds for licenses when deciding whether or not to grant a permit based on the expected thermal recovery efficiency. A quick analysis of licensed ATES systems in Flanders showed that currently about 75% of the systems are located in the Miocene aquifer system of which 75% are in the Diest Formation which was also targeted for this study. This underscores the practicality of the Darcy flux limits that were identified. For target aquifers that significantly deviate in characteristics from the ranges defined in the priors of this paper, conducting an additional sensitivity analysis may be required.

In the future, the results of the DGSA will be used as input for studies aiming to improve the design of shallow geothermal systems and to predict the uncertainty of their energy efficiency. For now, this uncertainty quantification is limited to the spreading around the general trend of increasing efficiency with smaller Darcy flux as illustrated in Figs. 5B and 8B. If there is no (reliable) flux measurement available or there cannot be certainty whether the proposed Darcy flux thresholds will be exceeded, a more advanced uncertainty quantification method should be used taking into account uncertainty on the sensitive parameters. In reality, at an early stage of exploration data is generally available from different sources, this data could be used to refine and update the prior and refine the DGSA (Lopez-Alvis et al. 2019). The available data should also be used to test the validity of the defined prior distribution by analyzing if the prior is able to generate output covering the available observations (Yin et al. 2020). After reducing the model complexity by fixing insensitive variables the prediction of the long-term behavior of ATES systems from short-term field tests becomes possible (Hermans et al. 2018). This will offer a thorough and accurate methodology for proper natural resource management and uncertainty quantification while handling the currently growing complexity of data and models as advocated by Ferré (2017).

## Conclusion

This study validates the use of a distance-based global sensitivity analysis for ATES systems. It shows that assumptions previously accepted with less general studies can also be demonstrated using a broad prior distribution and a DGSA. This supports that, when exploring a particular hydrogeological setting for ATES, it is beneficial to initially still consider the full uncertainty of the model parameters enhancing the generalizability of the results.

Specifically, this study provides a substantiated basis for fixing insensitive model parameters to average values in the studied hydrogeological settings. These parameters include the total and effective porosity, the longitudinal dispersivity, the recharge, and both vertical and horizontal hydraulic conductivity of the least permeable part of the aquifer. This study distinguishes itself from previous sensitivity analyses by showing that the uncertainty that will result from these simplifications can be viewed as the limited interval of thermal recovery efficiency values that are still considered possible if an accurate flux measurement is available (Figs. 5B and 8B).

The DGSA results also enhance our understanding of how surface temperature fluctuations impact the storage of thermal energy in very shallow aquifers. It proves that while these fluctuations do influence aquifer temperature and thus the ATES efficiency, model simplifications not accounting for soil temperature fluctuations are justified.

Furthermore, vertical thermal losses are counterbalanced by gains and they can be attributed to the functioning of the ATES system itself. This is a valuable outcome, indicating that, although methodologies exist to include all relevant heat transfer processes in the saturated and unsaturated shallow subsurface, it is not necessary to implement them in the context of ATES.

The parameters with major influence on the efficiency are the hydraulic conductivity, the natural hydraulic gradient and the annual storage volume. While this confirms the results of previous less general studies, this study further identifies Darcy flux thresholds that can serve when deciding upon the investment in ATES systems. In thick productive settings for ATES, a flux lower than 9.5 m/y indicates a very efficient system while a flux higher than 20.5 m/y characterizes the least favorable conditions. In shallow alluvial aquifers, ATES systems should not be implemented when Darcy fluxes are higher than 160 m/y because this will cause the system to be highly inefficient in terms of thermal recovery. As such, in a cost-efficient and logistically simple way, these flux measurements can provide a first measure of the ATES system's efficiency before carrying out a more detailed study.

For the two studied settings, new insights were also gained into the conditions where the recoverability of the stored thermal energy is optimal. A relatively low hydraulic conductivity and gradient will lead to a high recovery efficiency but these conditions are not a requirement. In this sense, flux measurements that account for both properties together, are more informative to identify favorable conditions.

In summary, this study shows that the DGSA method is effective in the context of ATES. It can serve to identify the sensitivity of model parameters, to reduce the model complexity without significantly reducing the uncertainty and to gain an understanding of the recovery efficiency and heat transport processes in different hydrogeological settings. This is crucial considering the tendency to target less known and less favorable aquifers and the aim for uncertainty quantification. The nuanced understanding gained from this study contributes to the optimization of ATES systems, offering practical guidance for more efficient feasibility studies and decision-making based on sound scientific approaches. The DGSA approach for ATES has great potential to explore new, more complex targets for ATES in a cost-effective way. Before field work is carried out, it can offer valuable insights into opportunities for streamlining models, optimizing field test selection, evaluating the potential for storage and establishing cutoff criteria for the investment. As such it can accelerate future development.

## Supplementary Information

The online version contains supplementary material available at https://doi.org/10.1186/s40517-024-00326-1.

Supplementary Material 1.

**Acknowledgements**

The resources and services used in this work were provided by the VSC (Flemish Supercomputer Center), funded by the Research Foundation—Flanders (FWO) and the Flemish Government. We would like to express our sincere thanks to the colleagues at KWR for their help with numerical problems and the warm welcome during a 2-month research stay. Finally, we truly appreciate the members of the DIAMONDS project team for the fruitful discussions and for offering new perspectives on the sustainable use of the subsurface.

**Author contributions**

LT: Conceptualization, Methodology, Software, Visualization, Data curation, Validation, Formal analysis, Investigation, Writing—original draft, Writing—review & editing, Funding acquisition. NH: Conceptualization, Methodology, Supervision, Writing—review and editing. MB: Conceptualization, Supervision, Writing—review and editing, Methodology. DS: Resources, Conceptualization, Supervision, Methodology, Writing—review and editing. TR: Resources, Writing—review and editing. RT: Software, Resources, Writing—review and editing. LZ: Methodology, Writing—review and editing. TH: Writing—review and editing, Supervision, Funding acquisition, Conceptualization, Methodology, Investigation, Formal analysis.

**Funding**
This work has received funding from the BOF (***bijzonder onderzoeksfonds***—special research fund) fellowship from Ghent University (grant number: 01D03222) and an FWO (Research Foundation Flanders) grant for a 2-month research stay at the KWR water research institute in Nieuwegein (The Netherlands) further promoted this research (grant number: V430223N). Later, Luka Tas became an SB (strategic basic research) PhD fellow, fully funded by FWO (grant number: 1SH0M24N). Further resources and services used in this work were provided by the VSC (Flemish Supercomputer Center), funded by the Research Foundation—Flanders (FWO) and the Flemish Government and the strategic basic research project DIAMONDS (grant number S001324N).

**Availability of data and materials**
The input and output data of the simulations generated and used for the DGSA's of this study are openly available on Zenodo https://doi.org/10.5281/zenodo.13347760. The scripts used to process the input and output are available on GitHub https://github.com/lukatas/ATES_SensitivityAnalyses.git (https://doi.org/10.5281/zenodo.13349645). The online version of the publication contains the supplementary material.

## Declarations

**Ethics approval and consent to participate**
Not applicable.

**Consent for publication**
Not applicable.

**Competing interests**
The authors declare no competing interests.

Received: 30 August 2024 Accepted: 4 December 2024
Published online: 07 January 2025

**References**

AGT (Advanced Groundwater Techniques). KWO potentieel in Vlaanderen: Kaart—Versie 3. AGTref.: 2015/C/01-1728-03 mp/jvs 09/10/15. Aartselaar: 2015.
Ajami H. Geohydrology: groundwater. In: Encyclopedia geology. Amsterdam: Elsevier; 2021. p. 408–15. https://doi.org/10.1016/B978-0-12-409548-9.12388-7.
Bakker M, Post V, Langevin CD, Hughes JD, White JT, Starn JJ, et al. Scripting MODFLOW model development using Python and FloPy. Groundwater. 2016;54:733–9. https://doi.org/10.1111/gwat.12413.
Batlle-Aguilar J, Brouyère S, Dassargues A, Morasch B, Hunkeler D, Höhener P, et al. Benzene dispersion and natural attenuation in an alluvial aquifer with strong interactions with surface water. J Hydrol. 2009;369:305–17. https://doi.org/10.1016/j.jhydrol.2009.02.014.
Bedekar V, Morway ED, Langevin CD, Tonkin MJ. MT3D-USGS: groundwater solute transport simulator for MODFLOW 2016. https://doi.org/10.5066/F75T3HKD.
Beernink S, Hartog N, Vardon PJ, Bloemendal M. Heat losses in ATES systems: the impact of processes, storage geometry and temperature. Geothermics. 2024;117: 102889. https://doi.org/10.1016/j.geothermics.2023.102889.
Beernink S, Barnhoorn A, Vardon P, Bloemendal M, Hartog N. Impact of vertical layering and the uncertainty and anisotropy of hydraulic conductivity on HT-ATES performance. 2022.
Bloemendal M, Hartog N. Analysis of the impact of storage conditions on the thermal recovery efficiency of low-temperature ATES systems. Geothermics. 2018;71:306–19. https://doi.org/10.1016/j.geothermics.2017.10.009.
Bloemendal M, Olsthoorn T. ATES systems in aquifers with high ambient groundwater flow velocity. Geothermics. 2018;75:81–92. https://doi.org/10.1016/j.geothermics.2018.04.005.
Bloemendal M, Jaxa-Rozen M, Olsthoorn T. Methods for planning of ATES systems. Appl Energy. 2018;216:534–57. https://doi.org/10.1016/j.apenergy.2018.02.068.
Bridger D, Allen D. Heat transport simulations in a heterogeneous aquifer used for aquifer thermal energy storage (ATES). Can Geotech J. 2010;47:96–115. https://doi.org/10.1139/T09-078.
Claesson J, Eskilson P. Conductive heat extraction to a deep borehole: thermal analyses and dimensioning rules. Energy. 1988;13:509–27. https://doi.org/10.1016/0360-5442(88)90005-9.
Compernolle T, Eswaran A, Welkenhuysen K, Hermans T, Walraevens K, Van Camp M, et al. Towards a dynamic and sustainable management of geological resources. Geol Soc Lond Spec Publ. 2022;528:101. https://doi.org/10.1144/SP528-2022-75.
Databank ondergrond vlaanderen (database underground flanders). Verkenner (Explorer) n.d. https://www.dov.vlaanderen.be/portaal/?module=verkenner. Accessed 10 Dec 2024.
Davies DL, Bouldin DW. A cluster separation measure. IEEE Trans Pattern Anal Mach Intell. 1979;1:224–7. https://doi.org/10.1109/TPAMI.1979.4766909.

De Paoli C, Duren T, Petitclerc E, Agniel M, Dassargues A. Modelling interactions between three aquifer thermal energy storage (ATES) systems in Brussels (Belgium). Appl Sci. 2023;13:2934. https://doi.org/10.3390/app13052934.

De Schepper G, Paulus C, Bolly P-Y, Hermans T, Lesparre N, Robert T. Assessment of short-term aquifer thermal energy storage for demand-side management perspectives: experimental and numerical developments. Appl Energy. 2019;242:534–46. https://doi.org/10.1016/j.apenergy.2019.03.103.

De Schepper G, Bolly P-Y, Vizzotto P, Wecxsteen H, Robert T. Investigations into the first operational aquifer thermal energy storage system in Wallonia (Belgium): what can potentially be expected? Geosciences. 2020;10:33. https://doi.org/10.3390/geosciences10010033.

Doughty C, Hellström G, Tsang CF, Claesson J. A dimensionless parameter approach to the thermal behavior of an aquifer thermal energy storage system. Water Resour Res. 1982;18:571–87. https://doi.org/10.1029/WR018i003p00571.

Duijff R, Bloemendal M, Bakker M. Interaction effects between aquifer thermal energy storage systems. Groundwater. 2021;61:173–82. https://doi.org/10.1111/gwat.13163.

Farmer WH, Vogel RM. On the deterministic and stochastic use of hydrologic models. Water Resour Res. 2016;52:5619–33. https://doi.org/10.1002/2016WR019129.

Fenwick D, Scheidt C, Caers J. Quantifying asymmetric parameter interactions in sensitivity analysis: application to reservoir modeling. Math Geosci. 2014;46:493–511. https://doi.org/10.1007/s11004-014-9530-5.

Ferguson G. Heterogeneity and thermal modeling of ground water. Groundwater. 2007;45:485–90. https://doi.org/10.1111/j.1745-6584.2007.00323.x.

Ferré TPA. Revisiting the relationship between data, models, and decision-making. Groundwater. 2017;55:604–14. https://doi.org/10.1111/gwat.12574.

Fleuchaus P, Godschalk B, Stober I, Blum P. Worldwide application of aquifer thermal energy storage—a review. Renew Sustain Energy Rev. 2018;94:861–76. https://doi.org/10.1016/j.rser.2018.06.057.

Fossoul F, Orban P, Dassargues A. Numerical simulation of heat transfer associated with low enthalpy geothermal pumping in an alluvial aquifer. Geol Belg. 2011.

Fu J, Jaime G-H. Uncertainty assessment and data worth in groundwater flow and mass transport modeling using a blocking Markov chain Monte Carlo method. J Hydrol. 2009;364:328–41. https://doi.org/10.1016/j.jhydrol.2008.11.014.

Gao L, Zhao J, An Q, Wang J, Liu X. A review on system performance studies of aquifer thermal energy storage. Energy Procedia. 2017;142:3537–45. https://doi.org/10.1016/j.egypro.2017.12.242.

Harbaugh AW, Langevin CD, Hughes JD, Niswonger RG, Konikow LF. MODFLOW-2005: USGS three-dimensional finite-difference groundwater model 2017. https://doi.org/10.5066/F7RF5S7G.

Hecht-Méndez J, Molina-Giraldo N, Blum P, Bayer P. Evaluating MT3DMS for heat transport simulation of closed geothermal systems. Groundwater. 2010;48:741–56. https://doi.org/10.1111/j.1745-6584.2010.00678.x.

Heldt S, Beyer C, Bauer S. Uncertainty assessment of thermal recovery and subsurface temperature changes induced by high-temperature aquifer thermal energy storage (HT-ATES): a case study. Geothermics. 2024;122: 103086. https://doi.org/10.1016/j.geothermics.2024.103086.

Hemmerle H, Ferguson G, Blum P, Bayer P. The evolution of the geothermal potential of a subsurface urban heat island. Environ Res Lett. 2022;17: 084018. https://doi.org/10.1088/1748-9326/ac7e60.

Hermans T, Nguyen F, Klepikova M, Dassargues A, Caers J. Uncertainty quantification of medium-term heat storage from short-term geophysical experiments using Bayesian evidential learning. Water Resour Res. 2018;54:2931–48. https://doi.org/10.1002/2017WR022135.

Hermans T, Lesparre N, de Schepper G, Robert T. Bayesian evidential learning: a field validation using push-pull tests. Hydrogeol J. 2019;27:1661–72. https://doi.org/10.1007/s10040-019-01962-9.

Hermans T, Goderniaux P, Jougnot D, Fleckenstein JH, Brunner P, Nguyen F, et al. Advancing measurements and representations of subsurface heterogeneity and dynamic processes: towards 4D hydrogeology. Hydrol Earth Syst Sci. 2023;27:255–87. https://doi.org/10.5194/hess-27-255-2023.

Hoffmann R, Dassargues A, Goderniaux P, Hermans T. Heterogeneity and prior uncertainty investigation using a joint heat and solute tracer experiment in alluvial sediments. Front Earth Sci. 2019;7. https://doi.org/10.3389/feart.2019.00108.

Hoteit H, He X, Yan B, Vahrenkamp V. Uncertainty quantification and optimization method applied to time-continuous geothermal energy extraction. Geothermics. 2023;110: 102675. https://doi.org/10.1016/j.geothermics.2023.102675.

Hughes JD, Langevin CD, Paulinski SR, Larsen JD, Brakenhoff D. FloPy workflows for creating structured and unstructured MODFLOW models. Groundwater. 2024;62:124–39. https://doi.org/10.1111/gwat.13327.

Jackson MD, Regnier G, Staffell I. Aquifer thermal energy storage for low carbon heating and cooling in the United Kingdom: current status and future prospects. Appl Energy. 2024;376: 124096. https://doi.org/10.1016/j.apenergy.2024.124096.

Jeon J-S, Lee S-R, Pasquinelli L, Fabricius IL. Sensitivity analysis of recovery efficiency in high-temperature aquifer thermal energy storage with single well. Energy. 2015;90:1349–59. https://doi.org/10.1016/j.energy.2015.06.079.

Kaufman L, Rousseuw PJ. Review of finding groups in data: an introduction to cluster analysis. 1990. https://doi.org/10.2307/2532178.

Klepikova M, Wildemeersch S, Hermans T, Jamin P, Orban P, Nguyen F, et al. Heat tracer test in an alluvial aquifer: field experiment and inverse modelling. J Hydrol. 2016;540:812–23. https://doi.org/10.1016/j.jhydrol.2016.06.066.

Kurylyk BL, MacQuarrie KTB, Caissie D, McKenzie JM. Shallow groundwater thermal sensitivity to climate change and land cover disturbances: derivation of analytical expressions and implications for stream temperature modeling. Hydrol Earth Syst Sci. 2015;19:2469–89. https://doi.org/10.5194/hess-19-2469-2015.

Lopez-Alvis J, Hermans T, Nguyen F. A cross-validation framework to extract data features for reducing structural uncertainty in subsurface heterogeneity. Adv Water Resour. 2019;133: 103427. https://doi.org/10.1016/j.advwatres.2019.103427.

Lu D, Ricciuto D. Efficient distance-based global sensitivity analysis for terrestrial ecosystem modeling. In: 2020 Int. Conf. Data Min. Workshop ICDMW, Sorrento, Italy: IEEE; 2020, p. 324–32. https://doi.org/10.1109/ICDMW51313.2020.00052.

Luo Z, Asproudi C. Subsurface urban heat island and its effects on horizontal ground-source heat pump potential under climate change. Appl Therm Eng. 2015;90:530–7. https://doi.org/10.1016/j.applthermaleng.2015.07.025.
Ma R, Zheng C. Effects of density and viscosity in modeling heat as a groundwater tracer. Groundwater. 2010;48:380–9. https://doi.org/10.1111/j.1745-6584.2009.00660.x.
Park J, Yang G, Satija A, Scheidt C, Caers J. DGSA: a Matlab toolbox for distance-based generalized sensitivity analysis of geoscientific computer experiments. Comput Geosci. 2016;97:15–29. https://doi.org/10.1016/j.cageo.2016.08.021.
Patton A, Cleall P, Cuthbert M. Identifying urban subsurface thermal and hydraulic processes from time-series groundwater temperature data. In: Copernicus Meetings; 2024. https://doi.org/10.5194/egusphere-egu24-1319.
Perzan Z. pyDGSA—a Python implementation of distance-based generalized sensitivity analysis (DGSA) 2020.
Possemiers M, Huysmans M, Batelaan O. Application of multiple-point geostatistics to simulate the effect of small-scale aquifer heterogeneity on the efficiency of aquifer thermal energy storage. Hydrogeol J. 2015;23:971–81. https://doi.org/10.1007/s10040-015-1244-3.
Poulsen SE, Balling N, Nielsen SB. A parametric study of the thermal recharge of low enthalpy geothermal reservoirs. Geothermics. 2015;53:464–78. https://doi.org/10.1016/j.geothermics.2014.08.003.
Preene M, Powrie W. Ground energy systems: from analysis to geotechnical design. Géotechnique. 2009;59:261–71. https://doi.org/10.1680/geot.2009.59.3.261.
Ramos-Escudero A, García-Cascales MS, Urchueguía JF. Evaluation of the shallow geothermal potential for heating and cooling and its integration in the socioeconomic environment: a case study in the region of Murcia. Spain Energies. 2021;14:5740. https://doi.org/10.3390/en14185740.
Renard P. Stochastic hydrogeology: what professionals really need? Groundwater. 2007;45:531–41. https://doi.org/10.1111/j.1745-6584.2007.00340.x.
Robert T, Hermans T, Lesparre N, De Schepper G, Nguyen F, Defourny A, et al. Towards a subsurface predictive-model environment to simulate aquifer thermal energy storage for demand-side management applications. In: Proc. SSB 2018 10th Int. Conf. Syst. Simul. Build., 2018.
Scheidt C, Li L, Caers J. Quantifying uncertainty in subsurface systems. 1st ed. New York: Wiley; 2018. https://doi.org/10.1002/9781119325888.
Schout G, Drijver B, Gutierrez-Neri M, Schotting R. Analysis of recovery efficiency in high-temperature aquifer thermal energy storage: a Rayleigh-based method. Hydrogeol J. 2014;22:281–91. https://doi.org/10.1007/s10040-013-1050-8.
Schweighofer JAV, Wehrl M, Baumgärtel S, Rohn J. Detecting groundwater temperature shifts of a subsurface urban heat island in SE Germany. Water. 2021;13:1417. https://doi.org/10.3390/w13101417.
Sommer W, Valstar J, van Gaans P, Grotenhuis T, Rijnaarts H. The impact of aquifer heterogeneity on the performance of aquifer thermal energy storage. Water Resour Res. 2013;49:8128–38. https://doi.org/10.1002/2013WR013677.
Stemmle R, Blum P, Schüppler S, Fleuchaus P, Limoges M, Bayer P, et al. Environmental impacts of aquifer thermal energy storage (ATES). Renew Sustain Energy Rev. 2021;151: 111560. https://doi.org/10.1016/j.rser.2021.111560.
Tas L, Simpson D, Hermans T. Assessing the potential of low-transmissivity aquifers for aquifer thermal energy storage systems: a case study in Flanders (Belgium). Hydrogeol J. 2023;31:2363–80. https://doi.org/10.1007/s10040-023-02696-5.
Wildemeersch S, Jamin P, Orban P, Hermans T, Klepikova M, Nguyen F, et al. Coupling heat and chemical tracer experiments for estimating heat transfer parameters in shallow alluvial aquifers. J Contam Hydrol. 2014;169:90–9. https://doi.org/10.1016/j.jconhyd.2014.08.001.
Winston RB. ModelMuse Version 5.1.1 2022. https://doi.org/10.5066/P90QQ94D.
Winter CL. Stochastic hydrology: practical alternatives exist. Stoch Environ Res Risk Assess. 2004;18:271–3. https://doi.org/10.1007/s00477-004-0198-0.
Yin Z, Strebelle S, Caers J. Automated Monte Carlo-based quantification and updating of geological uncertainty with borehole data (AutoBEL v1.0). Geosci Model Dev. 2020;13:651–72. https://doi.org/10.5194/gmd-13-651-2020.
Zeghici RM, Oude Essink GHP, Hartog N, Sommer W. Integrated assessment of variable density–viscosity groundwater flow for a high temperature mono-well aquifer thermal energy storage (HT-ATES) system in a geothermal reservoir. Geothermics. 2015;55:58–68. https://doi.org/10.1016/j.geothermics.2014.12.006.
Zhang L, Dieudonné A-C, Daniilidis A, Dong L, Cao W, Thibaut R, et al. Thermo-hydro-mechanical modeling of geothermal energy systems in deep mines: uncertainty quantification and design optimization. Appl Energy. 2025;377: 124531. https://doi.org/10.1016/j.apenergy.2024.124531.
Zuurbier KG, Hartog N, Valstar J, Post VEA, van Breukelen BM. The impact of low-temperature seasonal aquifer thermal energy storage (SATES) systems on chlorinated solvent contaminated groundwater: modeling of spreading and degradation. J Contam Hydrol. 2013;147:1–13. https://doi.org/10.1016/j.jconhyd.2013.01.002.

## Publisher's Note